Molecular Crystals and Liquid Crystals Science and Technology. Section A. Molecular Crystals and Liquid Crystals

Publication details, including instructions for authors and subscription information:
http://www.tandfonline.com/loi/gmcl19

AFM and Optical Investigations of Liquid Crystal Dewetting: Influence of Short and Long-Range Forces

Andreas Fery [a], Stephan Herminghaus [a] & Mohammed Ibn-elhaj [a]

[a] Max Planck Institut für Kolloid-und Grenzflächenforschung, Rudower Chaussee 5, D-12489, Berlin-Adlershof, Germany E-mail:

Version of record first published: 24 Sep 2006

To cite this article: Andreas Fery, Stephan Herminghaus & Mohammed Ibn-elhaj (1999): AFM and Optical Investigations of Liquid Crystal Dewetting: Influence of Short and Long-Range Forces, Molecular Crystals and Liquid Crystals Science and Technology. Section A. Molecular Crystals and Liquid Crystals, 330:1, 267-276

To link to this article: http://dx.doi.org/10.1080/10587259908025601

Mol. Cryst. Liq. Cryst., 1999, Vol. 330, pp. 267-276
Reprints available directly from the publisher
Photocopying permitted by license only

AFM and Optical Investigations of Liquid Crystal Dewetting: Influence of Short and Long-Range Forces

ANDREAS FERY, STEPHAN HERMINGHAUS
and MOHAMMED IBN-ELHAJ

Max Planck Institut für Kolloid- und Grenzflächenforschung, Rudower Chaussee 5 D-12489 Berlin-Adlershof, Germany; herminghaus@mpikg.fta-berlin.de

We have investigated the dewetting morphology of thin films of the liquid crystals $5AB_4$ and $5AB_3$, from a silicon substrate. For $5AB_4$, nucleation and spinodal dewetting can be clearly identified, and from scanning force microscopy of the liquid profiles, details of the effective interface potential can be quantitatively inferred. Due to peculiarities of the wetting forces in this system, the analogy to spinodal decomposition is particularly close. With $5AB_3$, an additional, rather complicated dewetting scenario is observed which is connected to the crystallization of droplets which have formed during the initial dewetting process.

INTRODUCTION

The various scenarios of structure formation in dewetting processes of thin liquid films have attracted growing interest in recent years [1-4]. However, despite the substantial amount of research in this direction, there are still many unsolved problems. This is mainly due to the difficulty of finding suitable model systems which permit the study of fundamental dewetting mechanisms in a well-controlled way. In the present paper, we report on observations of various dewetting modes in thin liquid crystal films. These appear to be promising model systems due to the large variety of similar, but slightly different, molecules available, which enables elucidative comparison of the dewetting modes of alike systems.

When a homogeneous liquid film is deposited onto a substrate which is not wet by the liquid, the film will rupture and dewet into an arrangement of sessile

liquid droplets forming a characteristic contact angle with the substrate at the contact lines. The most frequently encountered mechanism which initiates this process is the heterogeneous nucleation (e.g., at dust particles or other defects) of dry patches in the film. These evolve into steadily growing circular holes encompassed by (approximately) toroidal rims into which the removed material is accumulated. The spatial distribution of these holes is random, reflecting the random distribution of the nucleation centers at which they have formed [4]. Thermal nucleation usually does not play any significant role due to the high energies required for the initial hole formation.

This process of dewetting by nucleation has as its only requirement the finiteness of the contact angle, i.e., incomplete wetting. It is thereby irrelevant whether short range or long range forces are responsible for the contact angle to be finite. Theory predicts that there be an alternative dewetting mechanism which *requires the long range forces* to disfavour wetting. In this case, a wide spectrum of surface waves on the liquid (i.e., lateral fluctuations in film thickness) experience a driving force and thus grow exponentially in amplitude until the liquid surface reaches the substrate. This process does not require a nucleation barrier, and has been termed *spinodal dewetting* for its resemblance to the analogous scenario in decomposition processes of mixtures [5, 6]. We will demonstrate below that it may be observed in thin liquid crystal films, and that the dewetting morphology yields substantial insight into the microscopic interactions determining the wetting properties of the system.

DEWETTING OF 5AB$_4$

In particular, we have studied the behaviour of thin films of $5AB_4$ [7] (tris(trimethylsiloxy)silane-ethoxy-cyanobiphenyl) after transfer from a water surface onto a silicon wafer. This material undergoes a phase transition from the crystalline into the isotropic state at 18 °C. At room temperature (20 °C), three layers next to the substrate assume an alternately stacked, quasi-smectic arrangement [7], material farther away is isotropic. Films of $5AB_4$ were prepared by spreading the material from chloroform solution onto the surface of deionized water in a Langmuir trough at 10 °C. By surface compression, films with a typical thickness of $h = 40$ nm could easily be formed [7]. These films were transferred at a surface pressure of 6.9 mN/m onto silicon wafers which had been cleaned and hydrophilized by a modified 'RCA procedure' [8].

Fig. 1 shows an optical reflection micrograph of a film patch of $5AB_4$ directly after (a) and several minutes after (b) transfer to silicon. The irregular shape of the patches visible in fig. 1a suggests that the crystalline pancakes formed on the trough broke into pieces during transfer, such that there is no liquid crystal coverage to be expected in between the patches. As it is seen in Fig. 1b, the film dewets in the course of several minutes, involving mainly two dewetting

mechanisms. On the one hand, circular 'dry' holes appear, the dark rim of which is formed by the material removed from the hole. This is quite obviously due to nucleation from defects in the film, as it has been observed in a number of other systems [4, 9]. The rim of the patch also acts as a nucleation center, which gives rise to the observed retraction of the rim towards the patch center. Here, too, the removed material is being accumulated close to the retracting contact line, visible as a dark band close to the edge. On the other hand, there is dewetting by an undulative mode all over the patch, which exhibits a clearly defined critical wavelength, just as it is expected from spinodal dewetting. When the dewetting process is inspected through the microscope, one observes the nucleated dewetting to start almost immediately and to proceed gradually with time. In contrast, the undulative mode is not visible in the beginning, but appears after some time, then rapidly growing in amplitude until it reaches a 'final' state as shown in fig. 1b. This is consistent with what one expects for spinodal dewetting, i.e., for dynamically unstable surface waves.

That this system exhibits spinodal dewetting, may be qualitatively understood from the molecular interactions. The liquid crystal molecules are strongly dipolar, and thus a substrate with a high static polarizability favours the preparation of homogeneous films (complete wetting); otherwise there would be dewetting by the long range dipolar forces. It is therefore not surprising that it is possible to generate thick films on the Langmuir trough, due to the high polarizability ($\epsilon \approx 80$) of the water. The marked influence of the polarizability of the subphase on long range wetting forces has, among others, been nicely shown recently in experiments on wetting of pentane on water [10]. In contrast, when the film is transferred onto the silicon wafer, the substrate polarizability is decreased roughly by a factor of twenty, thus reducing considerably the polar adhesion to the substrate, rendering the long range tail of the wetting force negative. The result is the observed dynamical instability of the surface ripples which leads to the characteristic dewetting pattern displayed in fig. 1b.

It is important to note that the presence of this undulation, which appears to represent a fully developed dewetting structure, does not keep the circular holes from growing, nor the edge of the patch from receding: finally, the whole patch dewets into large droplets due to these receding fronts. The reason for this behaviour can be found if one images the liquid crystal profile by AFM [11], which provides the resolution necessary to resolve its fine structure. Fig. 2 shows a AFM image of a region close to the edge of a similarly generated dewetting structure, where the spinodal wave reached almost to the very edge. A steplike feature with a height of about 5 nm (arrow) can be clearly seen. This is readily interpreted as the edge of the abovementioned trilayer, which is known to be a particularly stable configuration for this system [7]. It furthermore corroborates the above assumption that there is no liquid crystal coverage between the patches deposited on the silicon substrate. The slope to the higher elevation

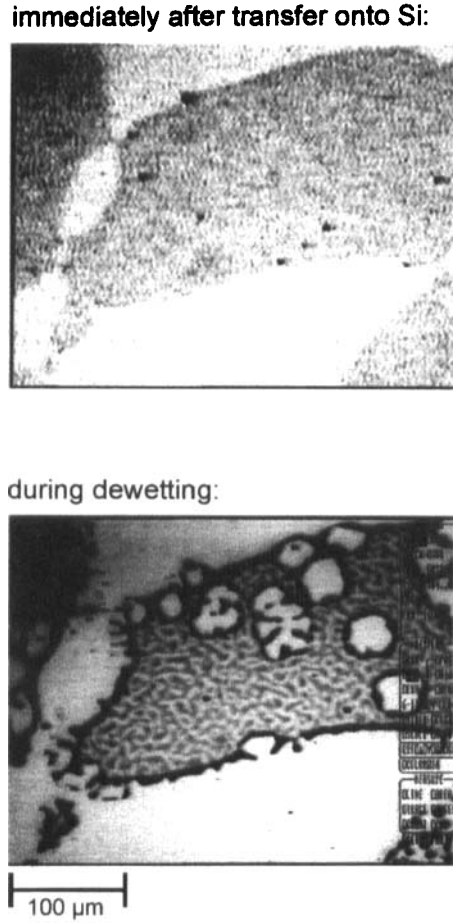

Figure 1: Dewetting of the liquid crystal film at room temperature after transfer to silicon: (a) immediately after transfer, (b) during dewetting. Nucleation of receding contact lines at defects and at the rims of the patch is observed as well as spinodal dewetting.

next to this step represents the receding edge of the liquid.

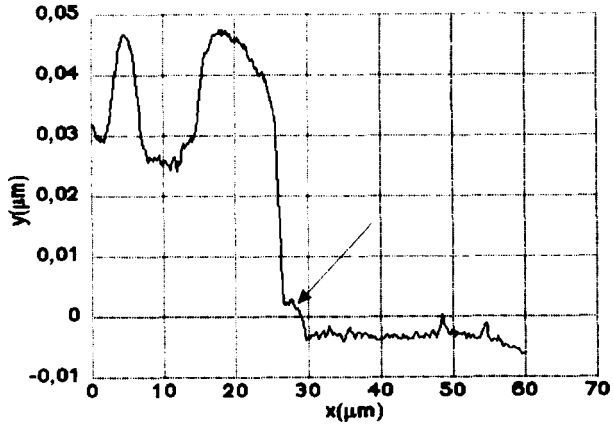

Figure 2: Scanning force image of the liquid crystal dewetting structure close to the rim of a patch. The 'valleys' of the undulation are at a much larger thickness (28 nm) than the stable trilayer, which corresponds to a thickness of 5 nm (arrow). This points to a local minimum in the effective interface potential, $\Phi(h)$, at $h = 25$ nm.

Farther to the left, two periods of the undulation are visible. Quite clearly, the minima of the undulation, which had at that point already reached a configuration steady enough for taking a AFM image, do in fact *not* represent the trilayer thickness, but instead a much larger thickness of about 28 nm. This seems to represent a metastable state of the system. It is now readily explained why a contact line reaching down to 5 nm thickness will recede even across a fully developed undulation, since there is still some energy to be gained.

The wetting behaviour of a liquid film is comprehensively described by the effective interface potential, $\Phi(h)$, of the film [12]. This is defined as the excess free energy which is required to approach the substrate/film interface and the film/air interface from infinity to the distance h (i.e., the film thickness). From the above observations, we can obtain quite accurate information about this important quantity. The smectic trilayer seems to represent the global minimum of $\Phi(h)$. A rough estimate for its depth can be obtained from the contact angle at the dewetting front, which is found to be 1.9 ± 0.4 degrees. For these small contact angles, the depth of the global minimum is given by $\frac{\sigma}{2}\tan^2\theta$ (where σ is the surface tension of the liquid), which yields $5.5 \pm 2.3 \times 10^{-4}\sigma$. Furthermore,

we know from the obvious instability of surface waves on the homogeneous patch that at the initial thickness of $h = 40$ nm, the second derivative of $\Phi(h)$ with respect to the film thickness, h, must be negative. More precisely, $\Phi''(h) = -8\pi^2\sigma/\lambda^2$ [13], where λ is the undulation wavelength, which we found to be 10μm in our case.

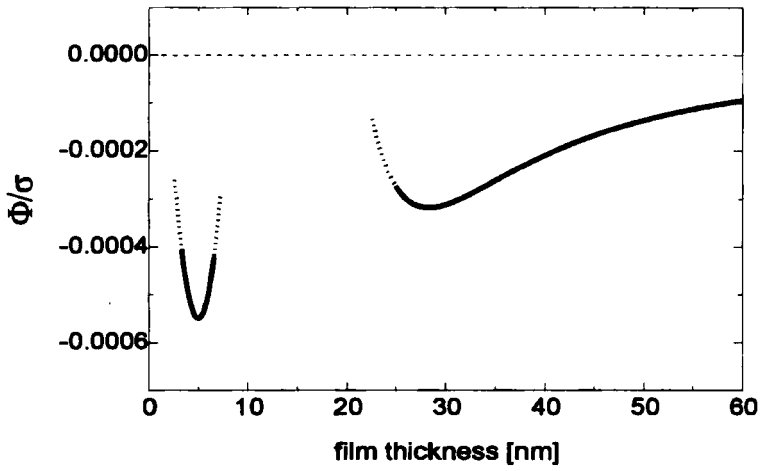

Figure 3: The effective interface potential, $\Phi(h)$, in units of the surface tension of the liquid, as inferred from the features in fig. 3. The long range tail, $\Phi \propto h^{-2}$, is adjusted such that its second derivative at $h = 40$ nm corresponds to the undulative wavelength of 10 μm found experimentally. The depth of its global minimum at 5 nm corresponds to the contact angle determined from cross sections of the liquid profile. The requirement of a local minimum at $h = 25$ nm leads almost inevitably to a large residual energy difference between Φ(25nm) and Φ(5nm), which provides the driving force for the continuation of dewetting even through the fully developed undulative dewetting structure.

Fig. 3 shows a sketch of $\Phi(h)$ as obtained from the above findings. Its long range tail is chosen to scale as $\Phi(h) \propto h^{-2}$, as expected for both nonretarded dispersive and dipolar forces, and scaled such that its second derivative at $h = 40$ nm corresponds to the undulative wavelength of 10μm. The requirement of a local minimum to appear at 25 nm leads almost inevitably to a substantial energy difference with respect to the global minimum at 5 nm, in accordance with the above observations. Although nothing can be said about the shape of $\Phi(h)$ in the regions indicated by the dotted lines, the solid lines can be

considered as quite reliable.

Recently, a ***stable*** (nematic) liquid crystal film of similar thickness has been observed, and the stability was interpreted as due to anchoring forces in the liquid [14]. However, our system is known not to exhibit nematic ordering [7], and thus we cannot ascribe the observed effect to director anchoring. On the other hand, spatial correlations in the isotropic phase may well come within the range of several molecular layers, even several degrees away from the phase transition temperature [15, 16], and thus give rise to the observed metastable film thickness. However, the precise nature of this stabilizing force remains to be clarified.

It is important to note that the presence of a shallow minimum close to the spinodal range renders this system particularly analogous to spinodal decomposition, where the binodal (representing a minimum in the free energy) appears close to the spinodal, stabilizing the concentration (the analogon of which is the film thickness, in our system) quite close to the value it had before the quench (here: to the initial film thickness)[17]. It is thus not astonishing that the undulative dewetting mode observed here has a striking resemblance to two-dimensional simulations of spinodal decomposition published earlier [17], in contrast to the spinodal dewetting morphology of gold films [6]. The latter system lacks a stabilizing force as the one found in the present system, and thus the undulations experience the full nonlinearity of the van-der-Waals force, with strong impact on the dewetting structure. A comprehensive comparison of these two systems is under way and will be published elsewhere.

DEWETTING OF $5AB_3$

With $5AB_3$, which has a smaller siloxane head group [7] and becomes isotropic at 53 °C, it is also observed that dewetting takes place from silicon substrates, leaving behind a rather stable trilayer plus a statistical ensemble of isolated droplets resting upon it. This state can be produced in a quite simple way by spin casting films from chloroform solution onto the silicon substrate, which immediately dewet within seconds. While the presence of the trilayer can be easily established by small angle X-ray reflectivity, inspection by optical microscopy reveals a statistical ensemble of droplets, the shape of which is perfectly spherical within the accuracy of observation.

At room temperature, this system is found to undergo another dewetting process, which we will call here secondary dewetting. It takes place usually several minutes after sample preparation and is different in its overall appearance from what is usually observed in dewetting liquid films. One observes that along an invisible 'line' (actually, a very elongated region) accross the sample, the droplets start to move while the others stay at rest. Fig. 4 shows a micrograph of this situation, with the moving droplets appearing somewhat blurred due to

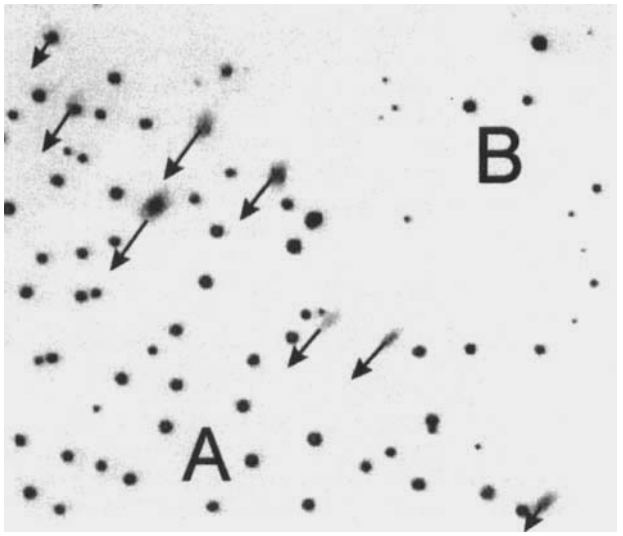

Figure 4: Optical micrograph of secondary dewetting of $5AB_3$ at room temperature. The droplets which are in motion can be identified by their appearing somewhat blurred due to the finite shutter time. The direction of their motion is indicated by the arrows. The elongated region in which droplets are moving separates the initial state (A, high density of spherical droplets) from the final state (B, low density of non-spherical droplets).

the finite shutter time. The elongated region of droplet motion, which separates region A from region B in the figure, wanders accross the entire sample. The droplets seem to follow this motion (arrows in the figure), thereby shrinking substantially and finally either vanishing or coming to rest again. This process leaves behind an ensemble of droplets of substantially reduced density and size, with individual droplets not being spherical anymore, but sometimes visibly faceted.

This latter obsrvation points to a crystallization of the droplets, and indeed, $5AB_3$ is known to be crystalline at room temperature [7]. Conversely, one may anticipate that before this process, the droplets are isotropic. In fact, the late stage clearly shows distinct peaks in the X-ray, while the initial stage does not. This leads us to the conclusion that at the initial stage, the material is supercooled and needs a seed to crystallize. Furthermore, one sees very clearly by

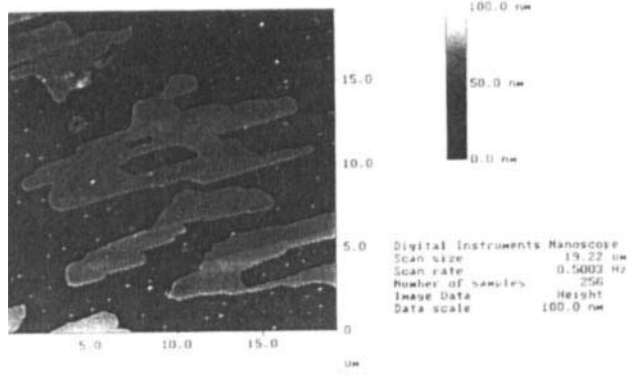

Figure 5: AFM image of a trace left behind by a droplet moving during secondary dewetting. The trace direction corresponds to the overall envelope of the mesas. The internal structure of the trace is obviously not aligned with the trace direction.

X-ray that while the droplets rest on a trilayer at the beginning (region A in Fig. 4), there is only a monolayer left at the final stage (region B). We thus arrive at the hypothesis that the whole process is driven by the dewetting of the upper bilayer (of the trilayer) from the lowest monolayer, which is thus left behind. This appears probable to happen, since X-ray reflectivity after the process reveals that the dominant layer period is considerably reduced with respect to the bilayer thickness, thus, the latter is not anymore a stable configuration. Furthermore, inspection of the process on an imaging ellipsometer showed clearly that a well defined front, invisible for the standard optical microscope, moves over the sample, and the contrast is consistent with what one expects for a reduction in film thickness by two molecular layers.

This model may also be used to explain the motion of the droplets. On the one hand, when the front of dewetting reaches a droplet, the latter 'sees' two different interfacial energies, corresponding to the trilayer at the leading edge and the monolayer at the trailing edge of the front. On the other hand, there is obviously an additional minimum in the effective interface potential (with respect to fig. 3) at a thickness of one monolayer, which is deeper than the one at the trilayer (otherwise, secondary dewetting would not take place). Consequently, the interfacial energy with the monolayer exceeds that with the

trilayer, which results in a force driving the droplet towards the trilayer region.

The fact that at the same time, the droplets crystallize, may be taken as evidence that the monolayer acts as an effective seed for the crystalline phase. One would thus expect that the droplets start to crystallize already during their motion. Indeed, closer examination of the final state by AFM reveals that every droplet leaves behind a trace of crystallized material, which is somewhat less wide than the respective droplet diameter, and has a rather uniform height of about 20 nm. The buildup of these structures explains directly why the droplets shrink during their motion. The majority of the material is being transformed into these traces upon the secondary dewetting process. They are internally well ordered, since distinct peaks appear in the X-ray reflectivity which correspond to an internal period less than the bilayer thickness, as mentioned above.

Fig. 5 shows an AFM image of such a trace, which is broken up into a substructure of individual patches. The fact that this substructure is not aligned with the trace direction points again to the crystallinity of the trace. Furthermore, the respective alignment of the patches over long distances yields evidence of quasi-epitactical crystallization upon the underlying monolayer, thereby corroborating the above assumption of the monolayer to act as a seed. We finally note that the trace must already be in the crystalline state when it is left behind by the droplet: if it were of the same phase as the drop, the interfacial energy between the (relatively thick) trace and the drop would be certainly much smaller than the interfacial energy between the drop and the trilayer. Thus, the drop would move towards the trace, in obvious contradiction to the observations.

Inspiring discussions with Karin Jacobs are gratefully acknowledged.

References

[1] G. Reiter, *Langmuir* **9**, 1344 (1993).
[2] A. Sharma and A.T. Jameel, *J. Coll. Interface Sci.* **161**, 190 (1993).
[3] M. Elbaum and S.G. Lipson, *Phys. Rev. Lett.* **72**, 3562 (1994).
[4] K. Jacobs, S. Herminghaus, K.R. Mecke, *Langmuir* **14**, 965 (1998).
[5] V.S. Mitlin. *J. Coll. Int Sci.* **156**, 491 (1993).
[6] J. Bischof, D. Scherer, S. Herminghaus, and P. Leiderer, *Phys. Rev. Lett.* **77**, 1536 (1996).
[7] M. Ibn-Elhaj, H. Möhwald, M.Z. Cherkaoui, R. Zniber, *Langmuir* **14**, 504 (1998).
[8] R. Riegler, M. Engel, *Ber. Bunsenges. Phys. Chem.* **95**, 1424 (1991).
[9] T.G. Stange, D.F. Evans, W.A. Hendrickson, *Langmuir* **13**, 4459 (1997).
[10] K. Ragil, J. Meunier, D. Broseta, J. Indekeu, D. Bonn, *Phys. Rev. Lett.* **77**, 1532 (1996).
[11] AFM of polar liquids has been demonstrated recently: S. Herminghaus, A. Fery, D. Reim, *Ultramicroscopy* **69**, 211 (1997), and T. Pompe, A. Fery, S. Herminghaus, *Langmuir* **14**, 2585 (1998).
[12] S. Dietrich in *Phase Transitions and Critical Phenomena* **12**, C. Domb and J.L. Lebowitz, eds.; Acad. Press, London (1988).
[13] E. Ruckenstein and R. K. Jain, Faraday Trans. **II 70**, 132 (1974).
[14] M.P. Valignat, S. Villette, J. Li, R. Barberi, R. Bartolino, E. Dubois-Violette, and A. M. Cazabat, *Phys. Rev. Lett.* **77**, 1994 (1996).
[15] B.M. Ocko, A. Braslau, P.S. Pershan, J. Als-Nielsen, M. Deutsch, *Phys. Rev. Lett.* **57**, 94 (1986).
[16] P.-G. De Gennes, *Langmuir* **6**, 1448 (1990).
[17] J.W. Cahn, *J. Chem. Phys.* **42**, 93 (1965).